Mechanical Suppression of SCC and Corrosion Fatigue Failures in 300M Steel Landing Gear

Paul Prevéy, President, Director of Research
N. Jayaraman, Director of Material Research
Lambda Technologies, 5521 Fair Lane, Cincinnati, OH 45227, 513.561.0883

Neal Ontko, Team Lead, Materials & Testing
Mike Shepard, AFRL/MLLMN
Robert Ware, Structural Failure Analysis
Jack Coate, Mechanical Engineer
Air Force Research Laboratory MLSC, 2179 12th Street, WPAFB, OH 45433

ABSTRACT

300M steel is widely used in landing gear because of its ultra high strength with high fracture toughness, but is vulnerable to both corrosion fatigue and stress corrosion cracking, with potentially catastrophic consequences. Plating and shot peening surface treatments currently used to extend life are only partly effective. A surface treatment is needed that will mitigate foreign object damage (FOD), corrosion fatigue and stress corrosion cracking. This paper describes the use of low plasticity burnishing (LPB) to improve damage tolerance and to mechanically suppress stress sensitive corrosion failure mechanisms.

The fatigue and corrosion fatigue performance of LPB processed 300M steel was compared with shot peened (SP) and low stress ground (LSG) conditions. LPB produced residual compression to a depth of 1.27 mm (0.050 in.), and shot peening only 0.127 mm (0.005 in.), an order of magnitude less. LPB treatment dramatically improved both the high cycle fatigue (HCF) performance and corrosion fatigue strength, with and without simulated FOD. LPB treated specimens with 0.020 in. deep FOD exhibited a definite endurance limit of 1035 MPa (150 ksi) even under corrosion fatigue conditions. Stress corrosion cracking (SCC) testing of LPB treated landing gear sections at 1030 to 2270 MPa (150 to 180 ksi) static loads was terminated after 1500 hrs without failure, compared to failure in as little as 13 hours without treatment. Corrosion and FOD caused early crack initiation and growth, dramatically decreasing fatigue performance. Deep surface compressive from LPB mitigated both the individual and synergistic effects of corrosion fatigue and FOD. LPB reduced the surface stress well below the SCC threshold for 300M, even under high tensile applied loads, effectively mechanically suppressing the SCC failure mechanism.

Future efforts will assess interactions with nickel and chrome plating, as well as the effects of compensatory tensile stresses.

Keywords: Residual Stresses, Surface Enhancement, Corrosion Fatigue, Stress Corrosion Cracking (SCC), High Cycle Fatigue (HCF), Low Plasticity Burnishing (LPB), Shot Peening (SP), Foreign Object Damage (FOD)

INTRODUCTION

SCC, corrosion fatigue, and FOD are generally recognized as significant degradation processes that effect aircraft landing gear components. Ultrahigh strength steels such as 4340, AF1410, and 300M are widely used in applications where a combination of high strength and fracture toughness is needed. Most of these ultrahigh strength steels have been known to be prone to SCC and corrosion fatigue.[1-4] The phenomenon of SCC is generally understood to be the result of a combination of susceptible material, corrosive environment, and tensile stress above a threshold, as illustrated in Figure 1. Earlier solutions to reduce the susceptibility to corrosion and the environment have included modifying the material (alloy chemistry), or the use of protective coatings. New alloys[2,3] like Aermet100, Custom250, Custom465, and Allvac240 have shown some improved resistance to SCC. Cadmium plating of the steel to retard corrosion and SCC have been standard practice for many landing gear systems[4]. In this paper, a novel approach of "mechanical suppression" of SCC and corrosion fatigue is

Proceedings of ASIP 2004
Nov. 29 – Dec. 2, 2004, Memphis, TN
(LT Paper 254)

presented. SCC is mitigated by introducing a layer of surface compression with LPB to maintain the net surface stress below the SCC threshold.

Introduction of residual compressive stresses in metallic components has long been recognized[5-8] to lead to enhanced fatigue strength. The fatigue strength of many engineering components is improved by shot peening (SP) or cold working, or as a by-product of a surface hardening treatment like carburizing/nitriding, physical vapor deposition, etc. Over the last decade treatments like LPB[9], laser shock peening (LSP)[10], and ultrasonic peening[11] have emerged that benefit fatigue prone engineering components to different degrees. In all surface treatment processes, key benefits are obtained when deep compression is achieved with minimal cold work of the surface.

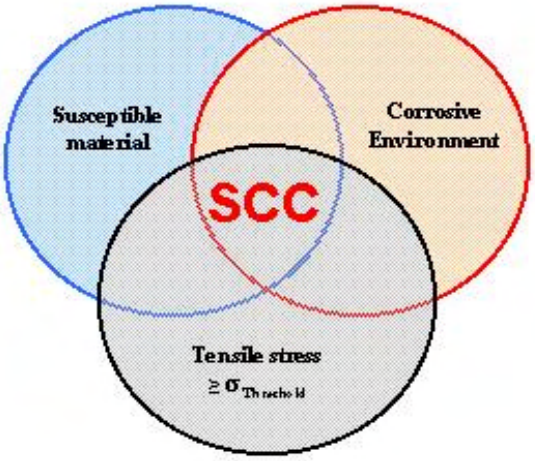

FIGURE 1 - SCC susceptibility diagram illustrating the need for the combination of a susceptible material, corrosive environment and threshold tensile stress to cause SCC.

LPB has been demonstrated to provide a deep surface layer of high magnitude compression in various aluminum, titanium, and nickel based alloys and steels. The deep compressive residual stress on the surface of these materials mitigates fatigue damage including FOD,[12-14] fretting,[15-16] and corrosion.[17-20] The LPB process can be performed on conventional CNC machine tools at costs and speeds comparable to conventional machining operations such as surface milling.
This research was undertaken to investigate the effect of a compressive surface residual stress state imparted by the LPB process upon the mechanisms of corrosion fatigue, damage tolerance and SCC in 300M steel, with comparison to a conventional SP surface treatment.

EXPERIMENTAL PROCEDURE

Material and Heat Treatment

300M steel was procured in the form of 0.5 in. (~12.7 mm) thick plates. Bars of nominal dimensions of 0.375 in. X 1.25 in. X 8 in. (9.5 mm X 31.75 mm X 203.2 mm) were initially machined. All bars were heat-treated to austenize at 1600ºF (871ºC) and oil quenched, followed by double tempering at 575ºF (302ºC) 8hrs + 8hrs and air cooling to room temperature.
The nominal composition and tensile properties of the heat-treated steel are as follows:

Chemical Composition: (weight%) C-0.41%, Mn-0.76%, P-0.007%, S-0.001%, Si-1.67%, Cr-0.73%, Ni-1.80%, Mo-0.38%, Al-0.040, Sn-0.005, Ti-0.001%, V-0.050, Cu-0.11, Bal-Fe.

0.2% Y.S. = 245 ksi (~1,690 MPa), UTS = 290 ksi (~2,000 MPa), Elong. = 10%, RA = 35%, HRC = 55HCF

Specimen Processing

Thick section fatigue specimens were finish machined from the heat-treated bars by LSG. A final heat treatment was performed after LSG. The fatigue specimens have a trapezoidal cross section in the gage region. This design enables the testing of specimens with a deep surface layer of compressive residual stress. The trapezoidal cross section HCF sample was designed to force the fatigue failures to initiate in the compressive gage section surface under 4-point bend loading.

LPB Processing

LPB process parameters were developed for thick sections of 300M steel using proprietary methods. The CNC control code was modified to allow positioning of the LPB tool in a series of passes along the gage section while controlling the burnishing pressure to develop the desired magnitude of compressive stress with relatively low cold working. Figure 2 shows a thick section fatigue specimen in the process of being LPB processed in the four-axis manipulator on the CNC milling machine.

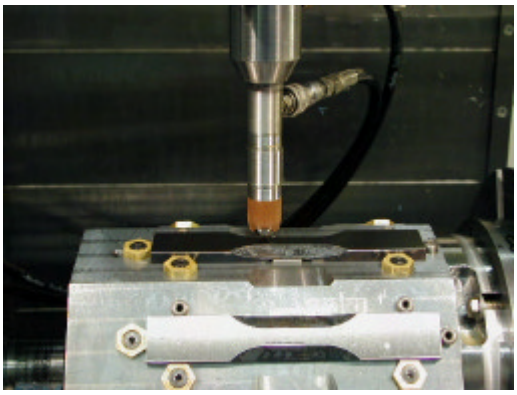

FIGURE 2 - A set of 8 thick section specimens being LPB processed in a 4-axis CNC milling machine.

SP Processing

Shot peening was performed using a conventional air blast peening system equipped with a rotating table on two sets of fatigue specimens with the following process parameters: 150% coverage and CCW14 shot; both 8A and 10A intensities were used for purposes of residual stress measurement, while only SP specimens with 10A intensity were used for fatigue testing. Residual stresses were measured in all surface treated specimens (both LPB processed and SP) before and after exposure to 400°F for 48 hours. The thermal treatment was selected to simulate an aggressive hydrogen bake-out used in landing gear production following cadmium or chromium plating, and allowed examination of any thermal relaxation of the compressive layer.

Residual Stress Measurement

X-ray diffraction residual stress measurements were made at the surface and at several depths below the surface on LPB treated fatigue specimens. Measurements were made in the longitudinal direction in the fatigue specimen gage employing a $\sin^2\psi$ technique and the diffraction of chromium Ká1 radiation from the (211) planes of steel. The lattice spacing was first verified to be a linear function of $\sin^2\psi$ as required for the plane stress linear elastic residual stress model[21-24].

Material was removed electrolytically for subsurface measurement in order to minimize possible alteration of the subsurface residual stress distribution as a result of material removal. The residual stress measurements were corrected for both the penetration of the radiation into the subsurface stress gradient[24] and for stress relaxation caused by layer removal.[25]

The value of the x-ray elastic constants required to calculate the macroscopic residual stress from the strain normal to the (211) planes of steel were determined in accordance with ASTM E1426-9.[26] Systematic errors were monitored per ASTM specification E915.

High Cycle Corrosion Fatigue Testing

All HCF tests were performed under constant amplitude loading on a Sonntag SF-1U fatigue machine. Fatigue testing was conducted at ambient temperature (~72F) in four-point bending mode. The cyclic frequency and stress ratio, R ($\sigma_{min}/\sigma_{max}$), were 30 Hz and 0.1 respectively. Tests were conducted to specimen fracture or until a "run-out" life of 2.5×10^6 was attained, whichever occurred first. Run-out specimens were subsequently re-tested to fracture at a minimum stress of at least 20 ksi greater than the stress level at which run-out had first occurred. For analysis purposes, such re-tests were regarded as virgin tests and results were included thus in S-N results. Cycling was terminated upon separation of the sample or when displacement resulting from severe cracking exceeded equipment limits. Specimens from tests terminated for the latter reason were subsequently broken open to permit direct observation of fracture surface details.

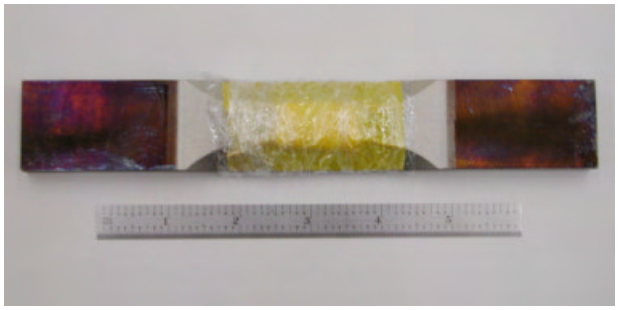

FIGURE 3 - A thick section specimen with 3.5% salt solution soaked tissue wrapped around the gage section.

Corrosion fatigue testing was performed in a medium of neutral 3.5% NaCl salt solution prepared with de-ionized water. Filter papers were soaked with the solution, wrapped around the gage section of the fatigue test specimen, and sealed with a plastic film to avoid evaporation. Figure 3 shows a specimen with the salt solution soaked filter paper sealed around the gauge section. To simulate FOD, a semi-elliptical surface notch of depth of a_o=0.020 in. (0.5 mm) and surface length of $2c_o$=0.060 in. (1.5 mm) was introduced in selected groups of specimens by electrical discharge machining (EDM),

as shown in Figure 4. Figure 5 shows the specimen mounted in the four-point bend fixture assembled for fatigue testing in a Sonntag SF-1U HCF machine. The following table describes the test conditions used in this study:

	Baseline (LSG)	Shot Peened	LPB Treated
Base (No FOD, No Salt)	✓	✓	✓
Salt Exposure	✓	✓	✓
Simulated FOD	✓	✓	✓
Simulated FOD + Salt Exposure	✓	✓	✓

Due to cumulative corrosion damage, re-testing at higher stresses was not performed on run-out specimens in corrosion fatigue tests.

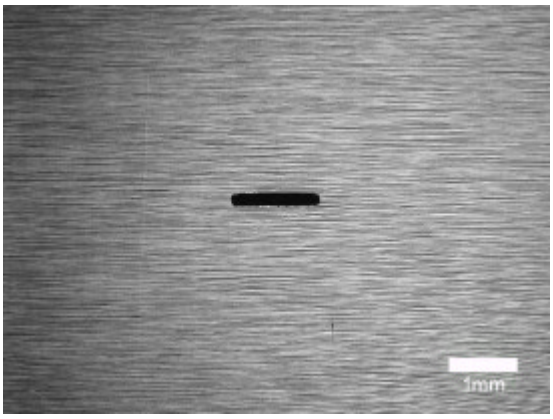

Figure 4a

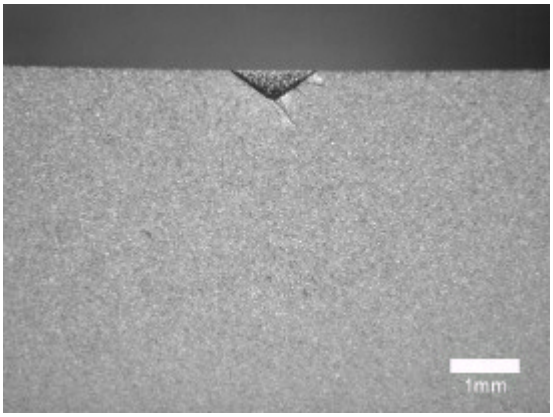

Figure 4b

FIGURE 4 - EDM notch to simulate FOD. (a) Top view, and (b) Cross-section of a 0.020 in. deep notch.

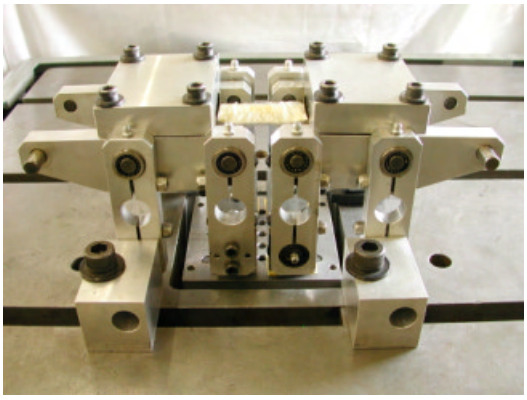

FIGURE 5 - Fatigue test set up.

Stress Corrosion Cracking Tests

SCC tests were performed on C-ring specimens (Figure 6) machined out of an actual landing gear made of 300M steel. The gage region of the C-ring specimen had a cross section similar to the fatigue specimens shown in Figure 2. This design made it possible to investigate the effect of surface treatments such as LPB for the SCC tests. Typically, when the specimen is loaded with a bolt through the ¾ in. (19 mm) hole, the outer surface of the trapezoid is in tension, and the tensile stress is nominally uniform over the 1 in. long parallel gage section. From the knowledge of the applied forces on the (instrumented) bolt, the bending moment and the corresponding tensile stress on the outer surface can be calculated. Three sets of specimens (both in an untreated condition and LPB treated) were SCC tested at 150, 165 and 180 ksi. The SCC test consisted of alternate immersion of the loaded specimen in a neutral 3.5% NaCl solution prepared with de-ionized water (10 min. in solution and 50 min. in air at room temperature). The load was monitored as a function of time, and the time to failure was noted.

Fractography

Following fatigue testing, each specimen was examined optically at magnifications up to 60x to identify fatigue origins and locations thereof, relative to the specimen geometry. Pictures were taken with a Nikon 990 digital camera through a Nikon Stereoscopic microscope at 15x. A representative photograph of a typical failure for each specimen group was obtained. A few selected specimens were also examined under a Cambridge S90B Scanning Electron Microscope (SEM).

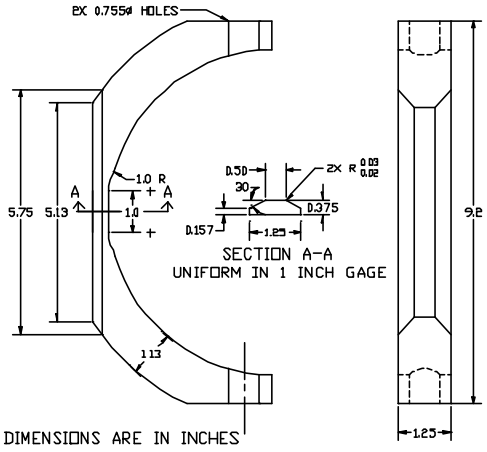

FIGURE 6 - C-ring specimen for SCC tests.

RESULTS AND DISCUSSION

Residual Stress Distributions

The residual stress distributions measured as functions of depth are presented graphically in Figure 7. Compressive stresses are shown as negative values, tensile as positive, in units of ksi (10^3 psi) and MPa (10^6 N/m^2). SP treatment at 8A intensity shows surface compression in the range of –100 to -115 ksi (-690 to -790 MPa), which becomes more compressive to about –150 ksi (-1035 MPa) at a depth of about 0.002 in. (0.05 mm), and rapidly relaxes to nearly zero at a depth of about 0.005 in. (0.125 mm). The 10A intensity of peening produced slightly deeper compression to a depth of 0.007 in. (0.18 mm). The residual stresses from both the SP treatments did not relax significantly after thermal exposure to 400°F for 48 hours. LPB treatment produces surface compression of -100 ksi (-690 MPa), increasing to about -180 ksi (-1240 MPa) at depths of 0.005 to 0.020 in. (0.125 to 0.5 mm), and gradually decreasing to zero at a depth of about 0.050 in. (1.25 mm). Again, thermal exposure to 400°F for 48 hours did not result in significant relaxation of residual stresses.

HCF and Corrosion Fatigue Performance

Figures 8-11 show the HCF and corrosion fatigue performance of 300M steel in the form of S-N curves. In Figure 8, the baseline material performance with and without the EDM notch and exposure to the corrosive environment is presented. The unnotched baseline condition shows a fatigue strength (endurance limit at 10^7 cycles) of nominally 150 ksi (1035 MPa). In the presence of a neutral 3.5% salt solution, the corrosion fatigue strength for baseline drops dramatically to only 30 ksi (205 MPa). Although the baseline material exhibited a strong endurance limit behavior, the endurance limit behavior was lost in the presence of salt solution, indicating further loss of strength with increasing time and cycles. Introduction of a semi-elliptical EDM notch 0.020 in. deep drastically decreases the fatigue strength to about 30 ksi (~140 MPa) in air, and to less than 10 ksi (70 MPa) in the salt solution. Power law lines were fitted to the data in Figure 8, and represent the average behavior of the material in its baseline condition.

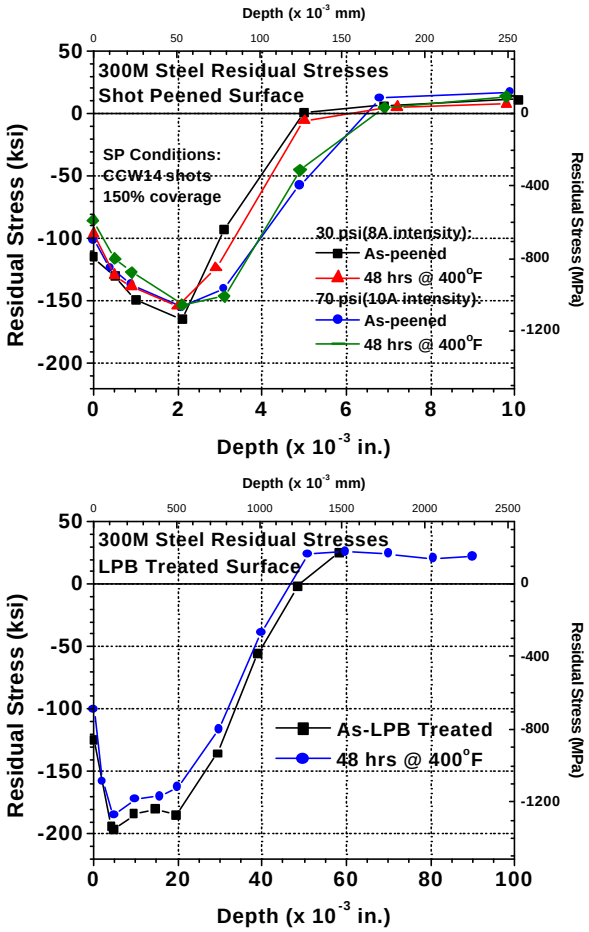

FIGURE 7 - Residual stress distribution for SP and LPB processed specimens. Thermal exposure at 400°F showed no significant effect on residual stresses.

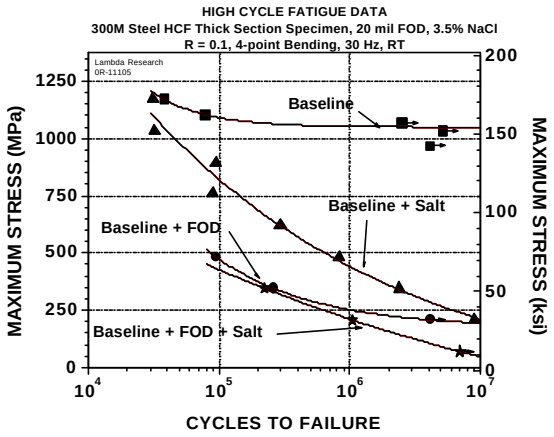

FIGURE 8 - Baseline fatigue results

Figure 9 shows the HCF and corrosion fatigue performance of both unnotched and notched SP treated specimens. Benefits of surface compression from the SP treatment are clearly seen in the improved HCF performance of the unnotched specimens. Corrosion fatigue strength in the presence of the neutral salt environment is reduced to nominally 75 ksi (515 MPa). This loss of fatigue strength, by a factor of 2, is not as severe as the factor of 5 debit seen in the baseline material. The small benefits of shallow compression from SP are evident in these results. However, the introduction of a 0.020 in. (0.5 mm) deep notch, exceeding the depth of the SP compressive layer, reduces the performance to essentially that the notched baseline condition both in air and in neutral salt.

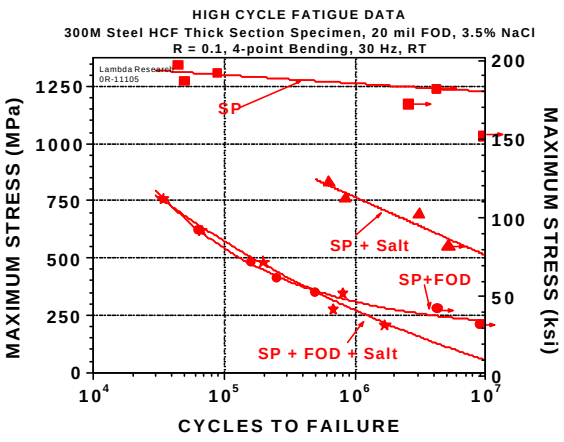

FIGURE 9 - Fatigue results for SP

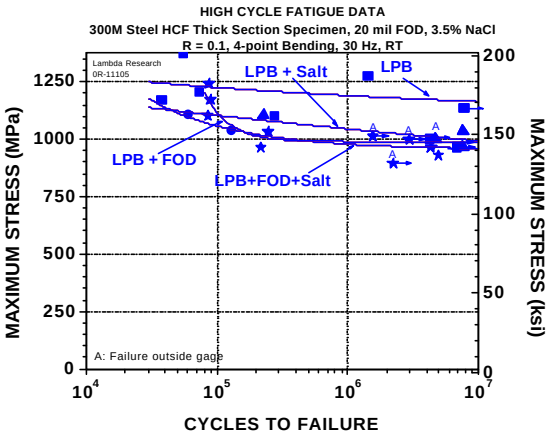

FIGURE 10 - Fatigue results for LPB

Figure 10 shows the HCF and corrosion fatigue behavior of LPB treated specimens. The unnotched specimen shows superior HCF performance, with a fatigue strength of 175 ksi (1200 MPa). Figure 10 also shows that fatigue data from all of the other test conditions with LPB treatments, notched HCF and both notched and unnotched corrosion fatigue test results, may be grouped into one set of data at a fatigue strength of 145 ksi (1000 MPa), just slightly lower than the baseline material. Three conclusions may be reached from this data. First, the LPB process has effectively mitigated corrosion fatigue. Second, the HCF and corrosion fatigue performance of this group is statistically similar to the unnotched baseline material. Third, the endurance limit behavior that was absent in both baseline and SP treatment when tested in the neutral salt solution environment is restored with the LPB treatment, an important finding for legacy aircraft operated at extended lives.

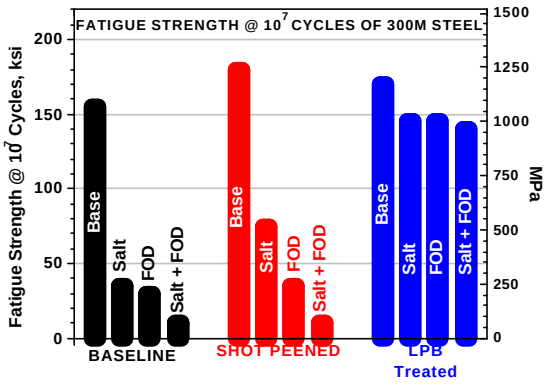

FIGURE 11 – Summary of Fatigue Results

Figure 11 shows a summary of HCF and corrosion fatigue test results. Here, it is evident that for both baseline and SP materials, a 0.020 in. (0.25 mm) deep EDM notch greatly decreases the HCF and corrosion fatigue strength to a value between 30 and 10 ksi (200 and 70 MPa). In contrast, the LPB treated specimens withstood the same EDM notch with a fatigue strength of 145 ksi (1000 MPa). Again, the HCF and corrosion fatigue performance for the LPB treated specimens are consistent with the residual stress distributions seen in Figure 7.

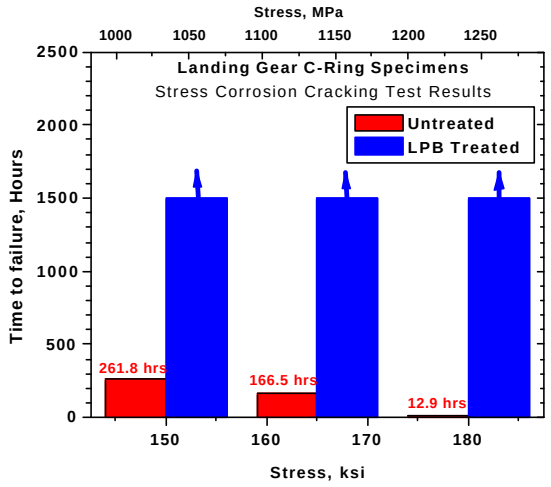

FIGURE 12 - SCC test results.

In Figure 12 the SCC test results show the untreated baseline material had SCC time to failure of 261.8 hrs at 150 ksi (1034 MPa), 166.5 hrs at 165 ksi (1138 MPa) and only 12.9 hrs at 180 ksi (1241 MPa), respectively. The LPB treated specimens did not fail even after 1500 hrs of exposure at all three stress levels. When the specimens were loaded to higher stress levels in an attempt to force SCC cracking, the specimens were severely bent without ever cracking. These results indicate the deep surface compressive stresses from LPB prevent the surface in contact with the corrosive environment from ever reaching the SCC threshold stress, thus fully mitigating SCC as a failure mechanism in 300M.

Fractography

Fractographic analyses presented here in Figures 13, 14 and 15 are limited to unnotched corrosion fatigue tested specimens with baseline, SP, and LPB conditions. Fractographic analyses of the notched and other HCF test conditions yielded results that are expected and consistent with the fatigue test results shown in Figures 8-11, and therefore are not further described. Figure 13a shows the fracture surface of a baseline specimen with a single crack initiation site near the corner of the trapezoidal cross-section. Figures 13b and c show the role of corrosion pits on the crack initiation process. Similarly Figures 14a, b and c, and Figures 15a, b, c and d show the optical fractographs, the gage of surface with corrosion pits, and the cross-sectional view of a corrosion pit in an unnotched SP and LPB specimen. In all cases, pitting of the gage surface is evident, and the cross-sectional views indicate a gradual increase in the depth of corrosion pitting damage with increased time of testing. In both baseline and SP specimens, the corrosion pits resulted in early crack initiation at low stresses, leading to final failure. In contrast, for LPB specimens, despite the higher stress levels and deeper corrosion pitting damage due to the longer exposure time during testing, the corrosion fatigue performance is minimally affected. This is seen in Figures 15a and b, where subsurface crack initiation is evident despite the presence of deep corrosion pits similar to the one seen in the cross-sectional view in Figure 15d.

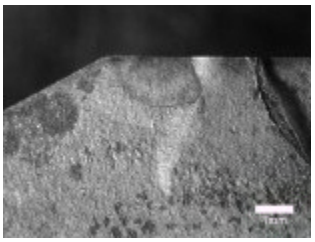

FIGURE 13a

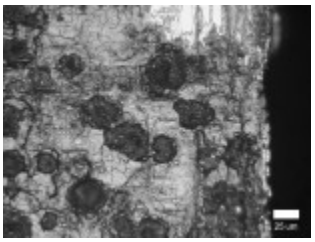

FIGURE 13b

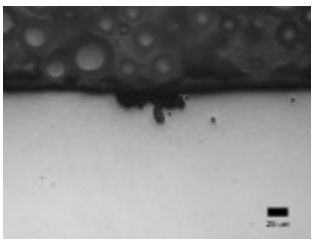

FIGURE 13c

FIGURE 13 - (a) Fracture surface showing crack initiation (arrow) from a corrosion pit, (b) gage surface of the specimen showing a typical set of corrosion pits, and (c) cross-sectional view of a typical corrosion pit in a corrosion fatigue tested baseline specimen; S/N 97, Smax=50 ksi, Nf=2.4(10^6) cycles (~24 hours)

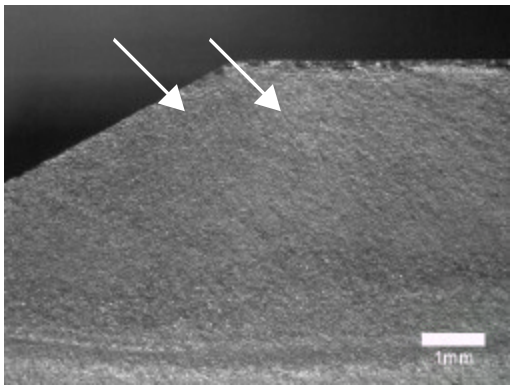

FIGURE 14A

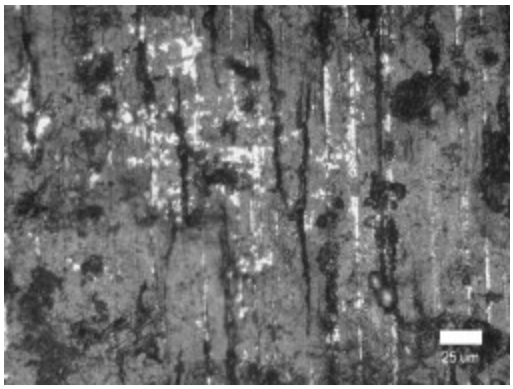

FIGURE 14b

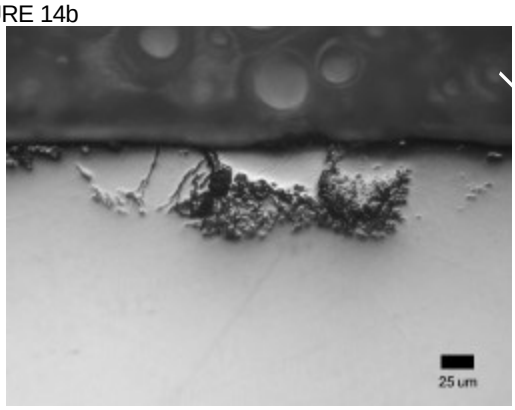

FIGURE 14c

FIGURE 14 - (a) Fracture surface showing multiple crack initiation (arrows) sites, (b) gage surface showing a set of typical corrosion pits, and (c) cross-sectional view of a typical corrosion pit in a corrosion fatigue tested SP specimen; S/N 94, Smax=100 ksi, Nf=3.1(10^6) cycles (~30 hours).

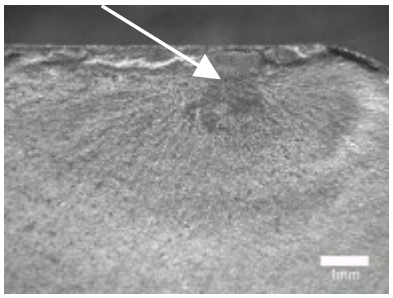

FIGURE 15a

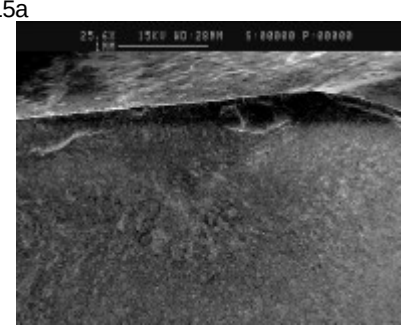

FIGURE 15b

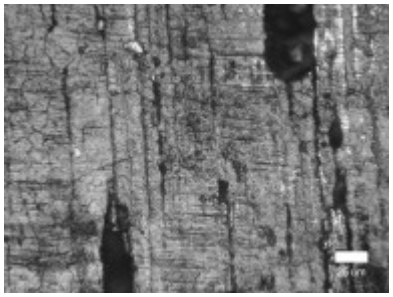

FIGURE 15c

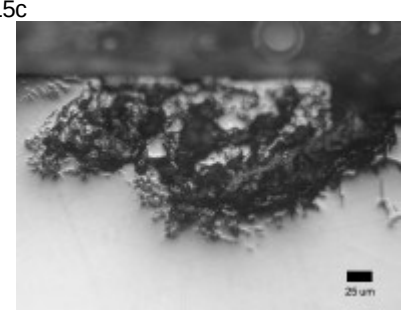

FIGURE 15d

FIGURE 15 - (a) Optical fractograph showing subsurface crack initiation (arrow) site, (b) SEM fractograph showing the same region, (c) gage surface corrosion pits and cracking, and (c) cross-sectional view of a typical corrosion pit in a corrosion fatigue tested LPB specimen; S/N 11, Smax=150 ksi, Nf=7.1(10^6) cycles (~70 hours)

CONCLUSIONS

The potential benefits of LPB treatment of 300M landing gear steel has been investigated and quantified in terms of corrosion fatigue performance and SCC in a neutral salt solution environment, and damage tolerance to a depth of 0.020 in. The performance with LPB treatment was compared to the baseline material performance and that of a conventionally shot peened surface. LPB introduced a layer of compression approaching the yield strength in magnitude and extending to 0.050 in. The LPB treatment effectively mitigated FOD up to 0.020 in. deep and eliminated the large fatigue debit caused by exposure to salt water. Because the LPB treated surface remains in compression even under high tensile applied loads, stress corrosion cracking was effectively entirely mitigated in salt water exposure.

The performance of LPB treated 300M steel demonstrated here supports the application of LPB to military and commercial aircraft landing gear with the combined potential benefits of reduced incidents of landing gear failure from either SCC or FOD, especially in salt water exposure, and potentially significant reductions in inspection maintenance requirements.

ACKNOWLEDGEMENTS

Support of this work by IR&D funds from Lambda Technologies and the Air Force Material Laboratory is gratefully acknowledged. The authors also wish to thank Doug Hornbach for residual stress measurements; Perry Mason and David Wright for conducting fatigue tests, and Brian Tent for SEM analysis.

REFERENCES

1. E. U. Lee, C. Lei, H.C. Sanders, R. Taylor, (2004), “Evolution of Fractograph During Fatigue and Stress Corrosion Cracking,” Naval Air Warfare Center, Aircraft Div Patuxent River Md, Report Number(S)- NAWCADPAX/TR-2004/12 Unclassified report.
2. E. U. Lee, (1995), Metall. Mater. Trans. A, 26A, (5); May, pp. 1313-1316.
3. Eun U. Lee, “Corrosion Behavior of Landing Gear Steels,” Naval Air Warfare Center Aircraft Div Warminster Pa Air Vehicle And Crew Syst Ems Technology Dept, Report Number - NAWCADWAR-94001-60 Unclassified report.
4. “High-Strength Steel Joint Test Protocol for Validation of Alternatives to Low Hydrogen Embrittlement Cadmium For High-Strength Steel Landing Gear and Component Applications”, (2003), July 31, Prepared by: The Boeing Company, Phantom Works, Seattle, Washington 98124, and Concurrent Technologies Corporation *(CTC*) Contract #CTC/LAU-CL2402-02 For: Air Force Research Laboratory Task Order 5TS5702D035M.
5. Frost, N.E. Marsh, K.J. Pook, L.P., (1974), *Metal Fatigue*, Oxford University Press.
6. Fuchs, H.O. and Stephens, R.I., (1980), *Metal Fatigue In Engineerin*g, John Wiley & Sons.
7. Berns, H. and Weber, L., (1984), "Influence of Residual Stresses on Crack Growth," Impact Surface Treatment, edited by S.A. Meguid, Elsevier, 33-44.
8. Ferreira, J.A.M., Boorrego, L.F.P., and Costa, J.D.M., (1996), "Effects of Surface Treatments on the Fatigue of Notched Bend Specimens," Fatigue, Fract. Engng. Mater., Struct., Vol. 19 No.1, pp 111-117.
9. Prevéy, P.S. Telesman, J. Gabb, T. and Kantzos, P., (2000), “FOD Resistance and Fatigue Crack Arrest in Low Plasticity Burnished IN718,” Proc of the 5th National High Cycle Fatigue Conference, Chandler, AZ. March 7-9.
10. Clauer, A.H., (1996), "Laser Shock Peening for Fatigue Resistance," Surface Performance of Titanium, J.K. Gregory, et al, Editors, TMS Warrendale, PA, pp 217-230.
11. T. Watanabe, K. Hattori, et al,, (2002), “Effect of Ultrasonic Shot Peening on Fatigue Strength of High Strength Steel,” Proc. ICSP8, Garmisch-Partenkirchen, Germany, Ed. L. Wagner, pg 305-310.
12. P. Prevéy, N. Jayaraman, R. Ravindranath, (2003), “Effect of Surface Treatments on HCF Performance and FOD Tolerance of a Ti-6Al-4V Vane,” Proceedings 8th National Turbine Engine HCF Conference, Monterey, CA, April 14-16.
13. Paul S. Prevéy, Doug Hornbach, Terry Jacobs, and Ravi Ravindranath, (2002), “Improved Damage Tolerance in Titanium Alloy Fan Blades with Low Plasticity Burnishing,” Proceedings of the ASM IFHTSE Conference, Columbus, OH, Oct. 7-10.
14. Paul S. Prevéy, et. al., (2001), “The Effect of Low Plasticity Burnishing (LPB) on the HCF Performance and FOD Resistance of Ti-6Al-4V,” Proceedings: 6th National Turbine Engine High Cycle Fatigue (HCF) Conference, Jacksonville, FL, March 5-8.
15. M. Shepard, P. Prevéy, N. Jayaraman, (2003), “Effect of Surface Treatments on Fretting Fatigue Performance of Ti-6Al-4V,” Proceedings 8th National Turbine Engine HCF Conference, Monterey, CA, April 14-16.
16. Paul S. Prevéy and John T. Cammett, (2002), “Restoring Fatigue Performance of Corrosion Damaged AA7075-T6 and Fretting in 4340 Steel with Low Plasticity Burnishing,” Proceedings 6th Joint FAA/DoD/NASA Aging Aircraft Conference, San Francisco, CA, Sept 16-19.
17. N. Jayaraman, Paul S. Prevéy, Murray Mahoney, (2003), “Fatigue Life Improvement of an Aluminum Alloy FSW with Low Plasticity Burnishing,”

Proceedings 132nd TMS Annual Meeting, San Diego, CA, Mar. 2-6.
18. Paul S. Prevéy and John T. Cammett, (2002), "The Influence of Surface Enhancement by Low Plasticity Burnishing on the Corrosion Fatigue Performance of AA7075-T6," Proceedings 5th International Aircraft Corrosion Workshop, Solomons, Maryland, Aug. 20-23.
19. John T. Cammett and Paul S. Prevéy, (2003), "Fatigue Strength Restoration in Corrosion Pitted 4340 Alloy Steel Via Low Plasticity Burnishing." Retrieved from www.lambda-research.com Sept. 5.
20. Paul S. Prevéy, (2000), "Low Cost Corrosion Damage Mitigation and Improved Fatigue Performance of Low Plasticity Burnished 7075-T6," Proceedings of the 4th International Aircraft Corrosion Workshop, Solomons, MD, Aug. 22-25.
21. Hilley, M.E. ed.,(2003), Residual Stress Measurement by X-Ray Diffraction, HS*J784*, (Warrendale, PA: SAE).
22. Noyan, I.C. and Cohen, J.B., (1987) Residual Stress Measurement by Diffraction and Interpretation, (New York, NY: Springer-Verlag).
23. Cullity, B.D., (1978) Elements of X-ray Diffraction, 2nd ed., (Reading, MA: Addison-Wesley), pp. 447-476.
24. Prevéy, P.S., (1986), "X-Ray Diffraction Residual Stress Techniques," *Metals Handbook*, **10**, (Metals Park, OH: ASM), pp 380-392.
25. Koistinen, D.P. and Marburger, R.E., (1964), Transactions of the ASM, **67**.
26. Moore, M.G. and Evans, W.P., (1958) "Mathematical Correction for Stress in Removed Layers in X-Ray Diffraction Residual Stress Analysis," SAE Transactions, **66**, pp. 340-345.